Microemulsions in oil-water-surfactant mixtures: Systematics of a lattice-gas model

Kan Chen, C. Ebner, and C. Jayaprakash
Department of Physics, The Ohio State University, Columbus, Ohio 43210

Rahul Pandit
Department of Physics, Indian Institute of Science, Bangalore 560012, India

A lattice-gas model is constructed for oil-water-surfactant mixtures. The phase diagram of this model is obtained by using mean-field theory and Monte Carlo simulations aided by low-temperature expansions. Microstructures, structure factors, and mean droplet lifetimes are also determined in some phases. Both two and three dimensions are studied, the former in more detail than the latter. It is shown that it is natural to interpret the paramagnetic phase in our model as a microemulsion. Our model is found to exhibit various properties that are in qualitative agreement with experimental observations of oil-water-surfactant mixtures: (1) two- and three-phase coexistence occurs between oil-rich, water-rich, and microemulsion phases along first-order phase boundaries or a triple line in certain regions of the phase diagram of our model; (2) the triple line, which ends in a tricritical point, is short and this leads to low oil-microemulsion and water-microemulsion interfacial tensions; (3) microstructures (including bicontinuous ones in three dimensions) and structure factors are similar to some experimental ones; (4) droplets in our microemulsion phase are long lived like their experimental counterparts; (5) long-lived, metastable phases, including long-period, lamellar, and glasslike phases, appear at low temperatures. The limitations of our model are discussed. Our study is compared with other studies of models of oil-water-surfactant mixtures.

I. INTRODUCTION

In this paper we study phase equilibria, static correlation functions, and some nonequilibrium properties in a lattice model that we have developed for the study of systems that exhibit microemulsion phases.[2-5] We begin this introduction with a survey of the experiments that have been done on these systems and a brief critique of current theories. We end with an overview of our principal results. In subsequent sections we present the details of our study.

A. Survey of experiments

Microemulsion phases occur in a class of three-component fluid mixtures,[6] in which there is a strong tendency for one of the components to be adsorbed at the interface between the remaining two components. The most common examples are oil-water-surfactant mixtures, such as mixtures of decane (oil), water, and AOT, i.e., sodium di-2-ethylhexyl-sulfosuccinate (surfactant).[6] Such mixtures exhibit a variety of phases because of two competing tendencies: (1) oil and water tend to phase separate, since the oil-water interfacial tension σ_{ow} is large ($\simeq 50$ dyn/cm); and (2) surfactant molecules, being amphiphilic, are adsorbed at an oil-water interface, so they tend to solubilize oil in water. (This adsorption lowers the bare oil-water tension σ_{ow} to values as low as 0.1 dyn/cm.[7]) The phases obtained are[2-5] (1) oil-rich phases (O); (2) water-rich phases (W); (3) lamellar phases (L) in which layers of oil and water are separated by layers of surfactant molecules [Fig. 1(a)];[8-11] (4) hexagonal phases (H) in which cylinders of oil (or water) are packed in a hexagonal array [Fig. 1(b)] in a water (or oil) background, with surfactant molecules at oil-water interface;[5] (5) microemulsion phases ($\mu\epsilon$) whose microstructure, though controversial (see below), is often pictured as small ($\simeq 100$ Å) droplets of oil in water [Fig. 1(c)] or water in oil [Fig. 1(d)], with surfactant molecules at oil-water interfaces; with comparable amounts of oil and water, the microstructure is envisaged as percolating, bicontinuous regions of oil and water separated by surfactant molecules [Fig. 1(e)];[2-5,12] (6) cubic crystalline phases (C), which are often made up of a complex arrangement of tubes, with water or oil cores and a sheath of surfactant molecules;[9,10] and (7) disordered, glasslike phases (G) whose structure and thermodynamic stability are not completely clear.[13]

Phase equilibria among the above phases have been studied experimentally for many years.[2-5] A rich variety of phase equilibria is found. Such phase equilibria are displayed typically in triangular phase diagrams, at constant temperature (Fig. 2). The details of such phases diagram very, of course, from system to system; however, these phase diagrams share the following qualitative features: (1) oil-rich (O) and water-rich (W) phases occur at low concentrations (up to a few percent by volume) of surfactant molecules; (2) microemulsion ($\mu\epsilon$) phases occur from low (a few percent by volume) to fairly high ($\simeq 80\%$ by volume) concentrations of surfactant molecules; (3) lamellar (L), hexagonal (H), and cubic (C) phases occur from medium (-20% by volume) to high (up to 100%) concentrations of surfactant molecules; and (4) both two-phase (O-W, O-$\mu\epsilon$, W-$\mu\epsilon$, W-L, L-H, H-C, etc.) and three-phase (O-W-$\mu\epsilon$, L-H-C, etc.) coexistence occur (Fig. 2). We refer the reader to the growing litera-

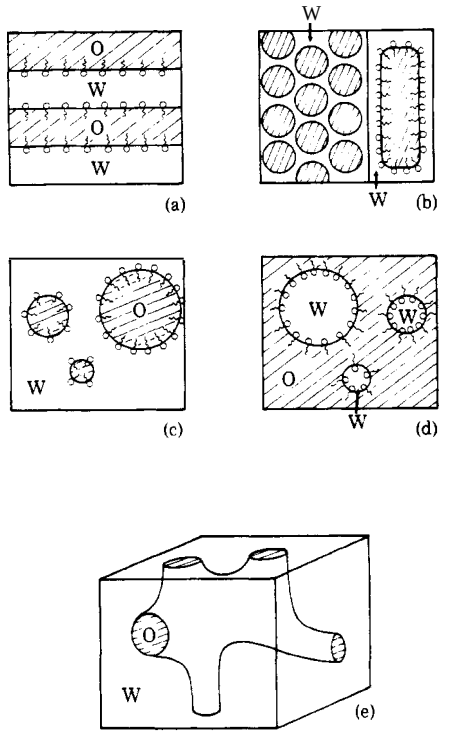

FIG. 1. Idealized microstructures for (a) a lamellar (L) phase, (b) a hexagonal (H) phase (a top view of the hexagonal array of cylinders and a side view of one cylinder are shown), and microemulsion ($\mu\epsilon$) phases with (c) droplets of oil in water, (d) droplets of water in oil, and (e) a bicontinuous structure. Shaded regions represent oil and unshaded regions, water. Surfactant molecules (shown with round heads and flexible tails) reside at oil-water interfaces [sometimes (e) they are not displayed for pictorial clarity].

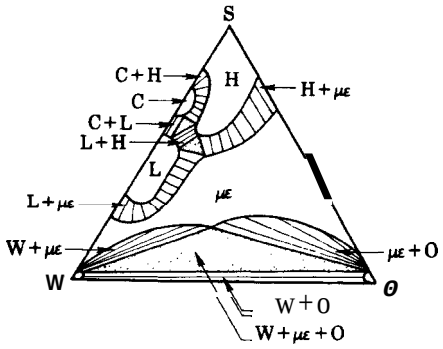

FIG. 2. Schematic phase diagram for an oil-water-surfactant (O-W-S) mixture in the composition triangle at fixed temperature. Unshaded areas represent single-phase regimes, areas hatched with tie lines indicate regions of two-phase coexistence, and dotted areas denote three-phase coexistence regions. Oil-rich, water-rich, microemulsion (με), lamellar (L), hexagonal (H), and cubic (C) phases are shown. In laboratory mixtures all these phases might not coexist as shown at one temperature; furthermore, different types of cubic, hexagonal, and lamellar phases might occur. The microstructure of the $\mu\epsilon$ phase varies from the oil-in-water type [Fig. 1(c)] near the water-rich corner, through the bicontinuous type [Fig. 1(e)] in the middle of the triangle, to the water-in-oil type [Fig. 1(d)] near the oil-rich corner.

ture[2-5,14-18] on experiments that trace the evolution of these phase diagrams as functions of temperature and the concentrations of other components (cosurfactants and electrolytes).[6] Critical points are also found in systems that exhibit microemulsion phases.

Light-scattering,[16,19-24] x-ray-scattering,[25-27] and neutron-scattering[28-33] studies yield the most reliable data on the microstructure of the preceding phases (Fig. 1). The oil-rich (O) and water-rich (W) phases are uniform liquids. The lamellar (L), hexagonal (H), and cubic (C) phases can be characterized, respectively, by the order parameters that describe conventional one-dimensional, two-dimensional, and three-dimensional crystals. To the best of our knowledge, detailed scattering studies have not been attempted in glasslike phases in these systems.

The interpretation of scattering data from microemulsion phases is not straightforward. Figures 3(a) and 3(b) show schematic plots of the sorts of structure factors that are found for microemulsion phases. If the static structure factor $S(k)$ has a peak at some nonzero value of $k = k_M$ [Fig. 3(b)], then k_M^{-1} can be identified as a characteristic length, such as a mean droplet size. However, a careful analysis of such structure factors shows that the same data can be fit by assuming that the microemulsion under investigation consists of a ***polydisperse*** system of ***spheres*** or a ***monodisperse*** system of ***ellipsoids*** of ***revolution.***[34] Nevertheless, the general belief, based on scattering[16,19-33] and other studies,[23,29,35,36] is summarized in the schematic diagrams Figs. 1(c)–1(e): at low concentrations of oil (water), microemulsions consist of ***polydisperse spheres*** of oil (water) in water (oil); when the concentrations of oil and water are comparable, a bicontinuous microstructure [Fig. 1(e)] is obtained.[37] Extended, cylindrical micelles have been reported in aqueous solutions of ionic surfactants.[38] However, it is not clear experimentally whether cylindrical microemulsions (i.e., microemulsions with cylindrical droplets) exist and are new phases that are distinct from spherical microemulsion phases (i.e., microemulsions with spherical droplets).[39]

The microstructures of microemulsions are not frozen in time: droplets and bicontinuous structures are in dynamic equilibrium. However, the typical lifetime of a

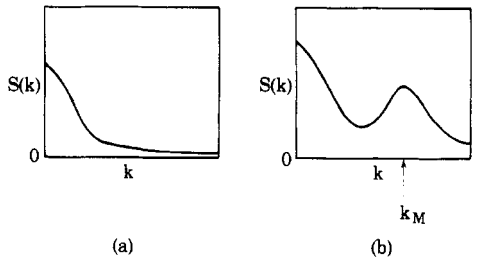

FIG. 3. Schematic plots of the structure factor $S(k)$ vs the magnitude of the wave vector $\mathbf{k}$ ($k = |\mathbf{k}|$) in the microemulsion phase. In some cases (a) $S(k)$ displays a maximum at $k = 0$; in others (b) $S(k)$ has an additional maximum at $k = k_M$ with $k_M^{-1} \simeq 100$ Å. For more detailed graphs see Ref. 31.

droplet[35,40] ($\simeq 10^{-6}$ s) is far greater than microscopic relaxation times in simple liquids ($\simeq 10^{-12}$ s).[41] Recent light-scattering measurements[42] have found a slow, non-Debye relaxation towards equilibrium in microemulsion phases.

Starting from potentials that describe the interactions between molecules of the three components of a microemulsion, a theory of phase transitions in systems with these three components must obtain the following: (i) the phases and their coexistence in such systems (Figs. 1 and 2), (ii) the static structure factors in these phases (Fig. 3), (iii) the equilibrium microstructures in these phases (Fig. 1), (iv) the mean times for which basic units (such as droplets) retain their identities in a given microstructure, (v) the modes of relaxation (perhaps non-Debye) to equilibrium in different phases, (vi) transport coefficients and response functions.

The theoretical tasks listed above are formidable, so theories have attempted only to explain some of the experiments outlined above. Some theories[1,12,43,44] have concentrated on microstructures, others[1,39,44–61] on phase equilibria in certain regions (say the region of low-surfactant concentration) of phase diagrams like the ones shown in Fig. 2, and yet others[52,61] on critical points in microemulsion phases; calculations of transport coefficients and response functions are in their infancy.[35] These theories are of two sorts: (1) continuum theories that start with phenomenological free energies[46–53] and (2) lattice theories that start with lattice-gas model ~ . ~ , ~Neither one of these two types of theories uses realistic potentials to describe the interactions between oil, water, and surfactant molecules. In addition, phenomenological theories either make *ad hoc* assumptions or approximations that cannot be controlled: e.g., one class of phenomenological theories[48–50] assumes that the mean size of droplets is an order parameter for the microemulsion phase; another phenomenological theory[52,62] uses an effective, attractive, droplet-droplet interaction to obtain critical points in microemulsion phases. Many studies of lattice models[55–59] make assumptions that imply, in effect, that microemulsion phases are periodically modulated.

B. Our model and principal results

Before we describe our lattice-gas model for oil-water-surfactant mixtures, we delineate briefly the reasons for adopting the statistical-mechanical approach we follow: we construct a simple, albeit incomplete, model for the oil-water-surfactant mixture; we analyze thoroughly the statistical-mechanical properties of this model (via mean-field theory and Monte Carlo simulations); thus we elucidate the ***minimal microscopic elements*** that a model must possess to yield various ***macroscopic properties*** (e.g., phase equilibria) of oil-water-surfactant mixtures. We find that our model, whose simple potentials mimic effectively (a) the tendency of oil and water to phase separate and (b) the tendency of surfactants to solubilize oil in water, displays various properties (see below) that are qualitatively similar to those of oil-water-surfactant mixtures. In addition, our study leads to new insights about such mixtures; in particular, it leads to insights about the nature of microemulsion phases.

Our lattice model does not use realistic molecular sizes or interactions. Nevertheless, the qualitative results we obtain from our study do have a bearing on the microscopic behavior of oil-water-surfactant mixtures. The principal advantage of using lattice models is that they are far easier to study in detail (via, say, Monte Carlo simulations) than continuum models: it is far easier to obtain reliably the phases, their microstructures, and phase boundaries for a lattice model than for a continuum model. We also note that phases of a continuum, fluid mixture can be qualitatively similar to phases of a (suitable) lattice model, as long as the densities of the components of the lattice model vary slowly (on the scale of the lattice spacing) in these phases. (Droplets and other structures in microemulsion phases are characterized by lengths that are much larger than molecular lengths, which can be taken to set the scale of the lattice spacing in a lattice model.)

Lattice models in general, and our model in particular, do suffer from some drawbacks in their description of fluid mixtures, such as oil-water-surfactant mixtures. We discuss them in detail in Sec. V. Because of these drawbacks, we have not tried to obtain all the phases that occur in oil-water-surfactant mixtures. Instead, we have concentrated on oil-rich, water-rich, and microemulsion phases, the phase boundaries between them, and their microstructures. Of course, we do find low-period lamellar and crystalline phases in our model; however, the relevance of these phases to those found in oil-water-surfactant mixtures is unclear.

We emphasize that we do not make any assumptions about the nature of microemulsion phases: we study the statistical mechanics of our model by using mean-field theory and Monte Carlo simulations in a way that places no restrictions on the spatial variation of the densities of oil, water, and surfactant molecules. Most of our calculations have been done for a two-dimensional version of our model. The principal qualitative points we make in this paper do not hold only in two dimensions. We have checked this by doing calculations for a three-dimensional version of our model.

We highlight now the most significant, qualitative results of our study. (1) In our model, we identify the microemulsion phase with the disordered phase (like a paramagnet, see below), for, in certain regions of our space of parameters, this disordered phase exhibits microstructures similar to those of laboratory microemulsions, although the surfactant concentration is surprisingly large compared to that in real systems (see Sec. V for discussion.) Furthermore, as the temperature increases, these microstructures evolve smoothly, without any intervening phase transitions, into microstructures that are characteristic of homogeneous and completely mixed solutions of oil, water, and surfactant molecules. This important result, which makes clear the nature of the microemulsion phase in our model, should be tested experimentally. By varying the pressure,[63] temperature, and the concentration of the constituents of a laboratory microemulsion, it should be possible to make it evolve

smoothly (no phase transitions) into a homogeneous and completely mixed solution of oil, water, and surfactant molecules. Of course, just as in the case of a liquid-gas transition, the evolution from low- to high-density phases might proceed via a first-order phase transition; however, there should be paths in parameter space (pressure, temperature, chemical potentials) along which this evolution should occur smoothly with no intervening phase transitions. (2) We find, as seen in experiments, a triple line along which oil-rich, water-rich, and microemulsion phases coexist. (3) This triple line ends in a multicritical point (a tricritical point). The triple line in our model is quite short (see below), thus all phases that coexist along it are in the vicinity of a tricritical point. Consequently, the interfacial tension between the microemulsion phase and the water-rich or oil-rich phases must be low (even though we have not calculated this explicitly).[64] By varying the temperature and the concentrations of the components of a microemulsion, especially the concentration of cosurfactant molecules, it should be possible to check experimentally for a tricritical point in the vicinity of the region of three-phase coexistence (O-W-$\mu\epsilon$ coexistence). Some evidence for such tricritical points and some critical end points already exists.[14] (4) We obtain the first microscopic theoretical example of a microemulsion that has a microstructure that can be truly described as random bicontinuous. Such a structure has previously been obtained from a cell model.[46]

In addition to T, the temperature, H, the difference of chemical potentials of oil and water, and μ, the chemical potential of surfactant molecules, our model (which we define precisely in Sec. II) has three parameters: (1) J, the strength of the oil-water interaction (we choose $J > 0$ in order to favor the phase separation of oil and water in the absence of surfactant molecules); (2) J_1, the strength of the surfactant-mediated oil-water interaction (we choose $J_1 < 0$ to favor the solubilization of oil in water); and (3) V, the strength of the surfactant-surfactant interaction (we allow $V > 0$ or $V < 0$, i.e., attractive or repulsive interactions). V can be thought of as an effective interaction in which the angular dependences have been averaged over. Very little is known about such interactions, so we investigate regions of parameter space where V is positive, negative, or zero. Unlike realistic potentials, all our potentials are short ranged; indeed, they are nearest-neighbor interactions in our lattice model. In some of our calculations we allow for next-nearest-neighbor interactions between surfactant molecules (Sec. II). In Sec. V we examine the consequences of using such approximate, short-range potentials.

In the following discussion, we sometimes use two symbols for a phase because, in Sec. II, we work with an Ising model that is equivalent to the lattice-gas model we are interested in. The second symbol refers to the nature of magnetic ordering in this equivalent Ising model.

We set the scale of energies by taking $J = 1$, explore the phase diagram of our model in the five-dimensional space of parameters J_1, V, T, H, and μ, and obtain microstructures and structure factors for various phases. Our principal results for our model are summarized below.

(i) At high temperatures our model displays a disordered phase (a paramagnet P) which we identify as a microemulsion ($\mu\epsilon$). In certain regions of our parameter space this phase displays an oil-in-water (Fig. 4) (or water-in-oil) microstructure, in other regions and in $d = 3$ it displays a bicontinuous microstructure. As the temperature rises, the sizes of different domains in these microstructures decrease, and they evolve ***smoothly, without any phase transition,*** into the microstructure of a conventional paramagnet.

(ii) At low temperatures we find the following phases: oil rich (O, i.e., ferromagnetic up $F+$); water rich (W, i.e., ferromagnetic down $F-$), low-period lamellar (LF+ and LF−, which are ferromagnetic, and LAF1 and LAF2, which are antiferromagnetic), low-period crystals (the antiferromagnetic phases AF1 and AF2), and uniform phases with a high density of surfactant molecules and a high density of oil or water (the ferromagnetic phases FS+ and FS−).

(iii) These phases coexist as shown in the schematic phase diagram of Fig. 5. [For simplicity we show only one three-dimensional section through the phase diagram in our five-dimensional parameter space; also, we restrict ourselves to our two-dimensional (spatial) model.] Note, in particular, that we obtain two- and three-phase coexistence between oil-rich, water-rich, and microemulsion phases (i.e., O-W, O-$\mu\epsilon$, W-$\mu\epsilon$, and O-W-$\mu\epsilon$; cf. Fig. 2, where densities vary and the temperature and the strengths of interactions do not, as in our phase diagrams).

(iv) In Fig. 6 we show the structure factor (oil water) of our model in a region of parameter space where a microemulsion phase exists. This should be compared with the structure factor of Fig. 3(a). We have not been able to find any region of parameters in our model in two dimensions where a structure factor like the one of Fig. 3(b) obtains.

(v) Our model displays many long-lived, metastable

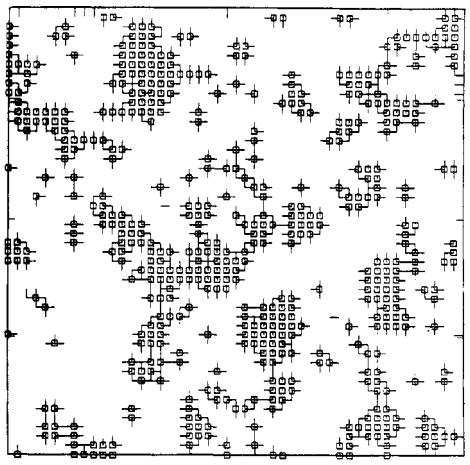

FIG. 4. Representative microstructure of the microemulsion phase obtained by Monte Carlo simulations of our model for two dimensions with $V_1 = 0$, $\mu = -1.0$, $H = -0.025$, $V = -0.1$, $J_1 = -2.6$, $T = 0.575$, and $J = 1$. The surfactant molecules are indicated by lines. The microstructures are the water (squares)-in-oil (empty spaces) type shown in Fig. 1(d).

phases, some of which are glasslike (i.e., disordered, but frozen on the time scale of our Monte Carlo simulations).

(vi) If we use single-spin-flip Glauber dynamics[65] in our Monte Carlo simulations, then the mean lifetime of a droplet in our microemulsion phase is 10^5–10^6 times the mean lifetime of a droplet in an Ising model with $T = 1.1T_c$, where T_c is the critical temperature of the Ising model. This enhancement of droplet lifetimes, compared to microscopic relaxation times in simple fluids, occurs in laboratory microemulsions.[35]

The remaining part of this paper is organized as follows: In Sec. I1 we define our model and determine its phase diagram in certain limits ($T = 0$ or $V = 0$), where it can be obtained either exactly or by the mapping of our model onto another model whose phase diagram is known, at least qualitatively. In Sec. III we study the phase diagram of our model by using mean-field theory. In Sec. IV we obtain the phase diagram of our model by doing Monte Carlo simulations; we also obtain microstructures and structure factors in our microemulsion phase. In Sec. V we list the limitations of our model, compare our results with those obtained from experiments, and compare our model with those of other groups.

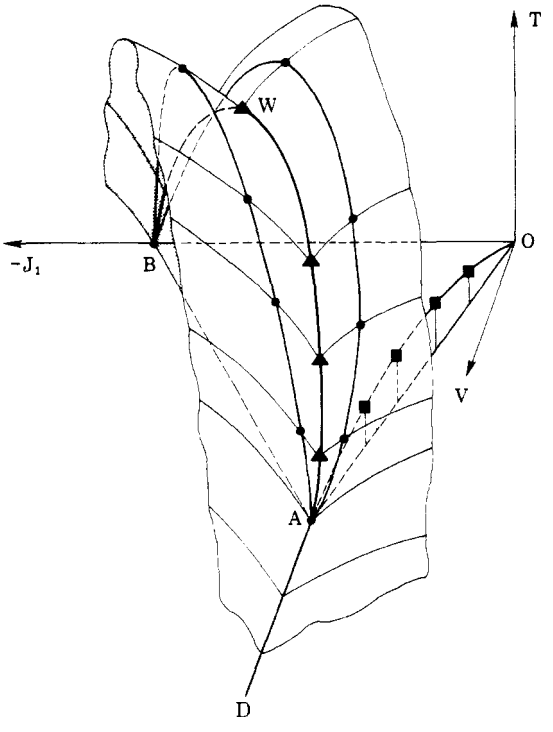

FIG. 5. Schematic phase diagram in two dimensions in V, J_1, and T space for $J > 0$, $V > 0$, $J_1 < 0$, $V_1 = 0$, and $H = 0$. Points O, A, B, and D are as in Fig. 9(a). There is a sheet of first-order transitions between the F and AF phases bounded by AB and the line of triple points (▲). Two sheets of first-order transitions branch off from the line (▲) and become sheets of critical phase transitions at the tricritical lines (●). These sheets separate the AS and F regions from the paramagnetic or microemulsion phase P at higher T; they drop to $T = 0$ on the line AD. Finally, there is a sheet of first-order transitions between the F and FS phases [see Fig. 9(a)] and bounded by the line OA and the line of critical points (■). The latter lies below the phase P everywhere except at A.

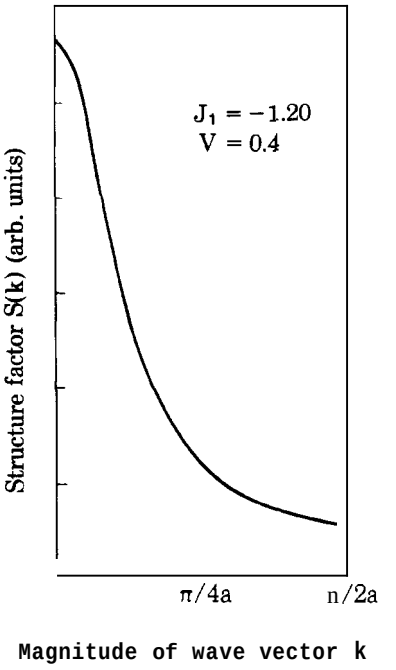

FIG. 6. Oil-water (partial) structure factor of our model for $J_1 = -1.20$, $V = 0.40$, and $T = 0.356$, where a microemulsion phase exists [cf. Fig. 3(a)]. Note that there is no subsidiary maximum. The width of the peak is larger than that for the Ising model at a comparable distance from the transition.

II. MODEL AND LIMITING CASES

Our model is a generalization of a model due to Alexander.[61] The Hamiltonian is

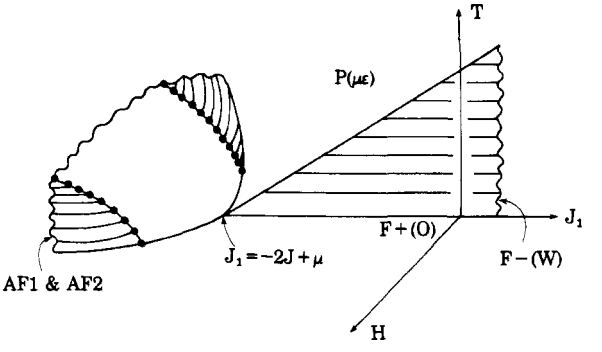

FIG. 7. Schematic phase diagram for Alexander's model in dimension $d > 1$ ($J = 1$). Shaded planes indicate first-order phase boundaries that terminate in critical lines (solid lines) or meet critical surfaces (unshaded) along lines of tricritical points (dot-dashed lines). Phase boundaries continue smoothly beyond the wavy lines at which they end in the figure. The ferromagnetic phases $F+$ (oil-rich) and $F-$ (water-rich) and the antiferromagnetic phases AF1 and AF2 evolve at high temperatures into the paramagnetic phase P which we interpret as a microemulsion ($\mu\epsilon$). Note that there is no first-order phase boundary along which oil-rich, water-rich, and microemulsion phases coexist.

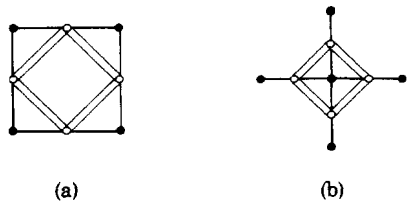

FIG. 8. Clusters of site (closed circles) and bond (open circles) variables used to determine the ground states of our model for (a) $V_1=0$ and (b) $H=0$ (see text).

$$\mathcal{H}=-H\sum_i \sigma_i - J\sum_{\langle i,j\rangle}\sigma_i\sigma_j - \mu\sum_{(i,j)}\tau_{ij} - V\sum_{\langle ij,ik\rangle}\tau_{ij}\tau_{ik} - V_1\sum_{\langle\langle ij,ik\rangle\rangle}\tau_{ij}\tau_{ik} - J_1\sum_{\langle i,j\rangle}\sigma_i\sigma_j\tau_{ij}\ , \tag{1}$$

where $\sigma_i=\pm 1$ occupy the sites i of a d-dimensional, hypercubic lattice and $\tau_{ij}=0,1$ occupy its links (ij); (i,j) are distinct, nearest-neighbor pairs of sites; and $\langle ij,ik\rangle$

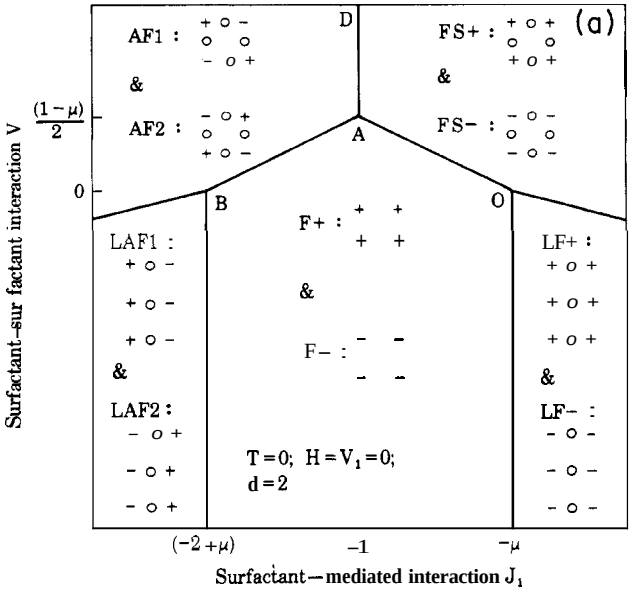

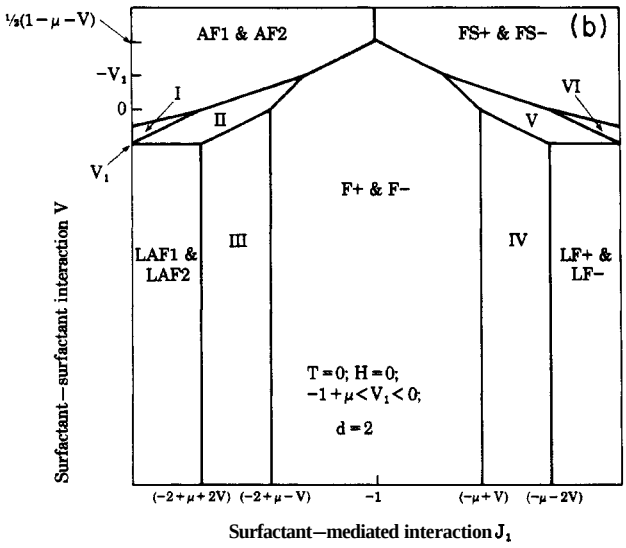

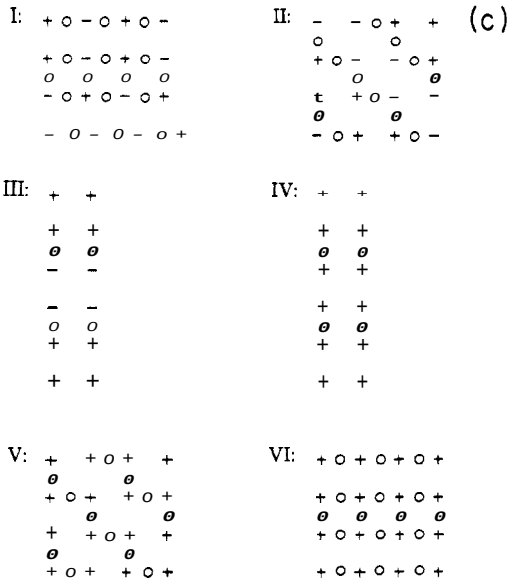

FIG. 9. Zero-temperature phase diagrams for model (1) in two spatial dimensions in the space of J_1 and V with $J=1$. Solid lines are first-order phase boundaries. (a) $H=V_1=0$. The structures of the phases in the different regions are shown explicitly with σ represented by $+$ or $-$; the presence of a surfactant is indicated by an open circle (see text). (b) $H=0$ and $-1+\mu<V_1<0$. Phases that appear at $V_1=0$ (a) are denoted by the same abbreviations. Note that six new phases appear (indicated by Roman numerals) whose microstructures are displayed in (c).

and $((ij, ik\rangle\rangle$ are, respectively, distinct pairs of links that meet at sites i at 90° and 180". We associate the Ising spin $\sigma_i = +1\,(-1)$ with the presence of an oil (a water) molecule at site i; thus, the field H is related directly to the difference between the chemical potentials of oil and water; the exchange interaction J is chosen to be positive so that it favors the phase separation of oil and water.[66] We associate $\tau_{ij} = 1\,(0)$ with the presence (absence) of a surfactant molecule on link $\langle ij\rangle$, μ is the chemical potential of surfactant molecules, and V and V_1 are used to parametrize the interactions of these molecules. J_1 is the strength of the surfactant-mediated interaction between nearest-neighbor Ising spins; we choose $J_1 < 0$ since it favors an antiferromagnetic alignment of nearest-neighbor spins σ_i and σ_j (if $\tau_{ij} = 1$); i.e., $J_1 < 0$ favors the solubilization of oil in water in the presence of surfactant molecules.

For $V = V_1 = 0$, the model (1) reduces to the one proposed by Alexander.[61] As he noted, in this case the partition function of this model is the same as that of the d-dimensional Ising model on a hypercubic lattice with an effective coupling

$$J_{\text{eff}} = J + \frac{1}{2\beta}\ln[(1+e^{\beta(J_1+\mu)})/(1+e^{-\beta(J_1-\mu)})] \qquad (2)$$

($\beta = 1/k_B T$, where k_B is the Boltzmann constant) between nearest-neighbor spins and with a field H acting on every spin. (This follows by summing over the τ_{ij}'s, an operation that is referred to as decimation or dedecoration.) Thus, in the limit $V = V_1 = 0$, the phase diagram of model (1) follows from the phase diagram of the equivalent Ising model described above.

Figure 7 shows a schematic phase diagram for model (1) with $V = V_1 = 0$, $\mu = 0$, and $d > 1$. (For $H = O$ and $d = 2$ the model can, of course, be solved exactly.[66]) Similar phase diagrams obtain for $\mu \neq 0$. Alexander's model has the phases we want to describe: two ferromagnetic phases $F+$ (oil-rich O) and $F-$ (water-rich W) and the paramagnetic phase P (microemulsion $\mu\epsilon$).[67] However, his model does not exhibit important, qualitative features that are present in experimental phase diagrams of oil-water-surfactant mixtures: in particular, it does not show first-order phase boundaries along which there is two-phase (O-$\mu\epsilon$, W-$\mu\epsilon$) and three-phase (O-W-$\mu\epsilon$) coexistence between oil-rich, water-rich, and microemulsion phases.

To overcome this failure of Alexander's model, we let V and V_1 be nonzero in model (1). Now it is not easy to obtain the phase diagram of this model, for it cannot be mapped onto an Ising model with interactions between nearest-neighbor spins. We describe below how we obtain the phase diagram in the limit $T = 0$. In this limit, all we have to do is to find the configuration of σ_i's and τ_{ij}'s that yields the lowest minimum of $\mathcal{H}$ [Eq. (1)].

At zero temperature ($T = 0$) we use Karl's method[68] to obtain exactly the phase diagram of model (1) for two cases: (a) $V_1 = 0$ and all other couplings arbitrary and (b) $H = 0$ and all other couplings arbitrary. In case (a) [case (b)] the minimization of H with respect to the σ_i's and τ_{ij}'s reduces to the problem of the minimization of the energies of the finite cluster of σ's and τ's shown in Fig. 8(a) [Fig. 8(b)]. The ground-state configuration of σ_i's and τ_{ij}'s, that gives the lowest minimum of H, is obtained by repeating periodically the lowest-energy configuration of the finite cluster (Fig. 8). All zero-temperature phase boundaries are first-order boundaries (Figs. 9 and 10); they are found by determining the loci of points along which the lowest minimum of $\mathcal{H}$ has an n-fold degeneracy, with $n \geq 2$.

In Fig. 9 (Fig. 10) we show representative, two-dimensional sections through the zero-temperature phase diagram of model (1) for $d = 2$ ($d = 3$). In addition to the zero-temperature phases of Alexander's model (Fig. 7), we find low-period (up to period 4) lamellar and superantiferromagnetic phases. A richer variety of phases appears for $d = 3$ (Fig. 10) than for $d = 2$ (Fig. 9). We have not studied the zero-temperature phase diagram in detail

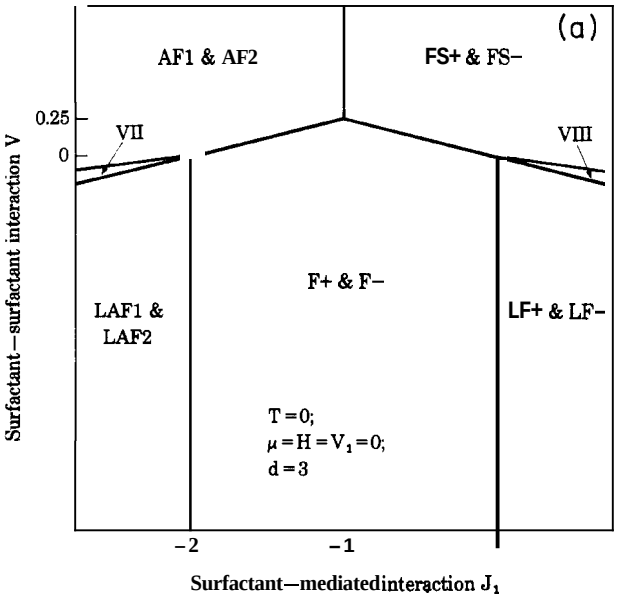

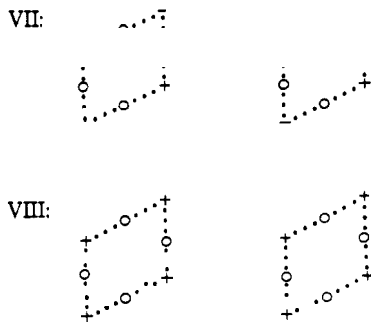

FIG. 10. Zero-temperature phase diagram for model (1) in $d = 3$ with $\mu = H = V_1 = 0$. The phases AF1, AF2, LAF1, LAF2, $F+$, $F-$, FS+, FS−, LF+, and LF− have microstructures which are the natural three-dimensional analogs of the corresponding d = 2 structures displayed in Fig. 9(a). The structures of the phases denoted by VII and VIII are shown in (b).

V_1 and H are nonzero. We have tried to find ground states in this case via slow, Monte Carlo annealing;[69] this has not yielded long-period lamellar or superantiferromagnetic ground states; however, given the complexity of our model, we cannot rule out the existence of such ground states when V_1 and H are both nonzero.

Along some of the zero-temperature phase boundaries in Figs. 9 and 10, many more phases coexist than are shown; e.g., in Fig. 9(a) ($d=2$, $T=H=V_1=0$, $J=1$) the ground state is infinitely degenerate (in the thermodynamic limit) in the following regions: (1) along the line $J_1=-1$, $V\geq(1-\mu)/2$ the *total* ground-state entropy $S(T=0)\sim N$, where N is the number of lattice sites; and (2) along the line $J_1=-2+\mu$, $V<0$, $S(T=0)\sim\sqrt{N}$; at the point $J_1=-2+\mu$, $V=0$, $S(T=0)\sim N$.

Zero-temperature phase boundaries, along which the ground state of a model is infinitely degenerate, are of potential importance: Thermodynamically stable, long-period phases often emerge from such phase boundaries (lines and points in Figs. 9 and 10) at nonzero temperatures in models with competing interactions.'' Such long-period phases do not always emerge from infinitely degenerate lines and points in the zero-temperature phase diagram of a model. In some models, infinitely degenerate ground states lead to a completely disordered phase (a paramagnet) at any $T>0$. In Secs. III and IV we use mean-field theory and Monte Carlo simulations to determine for model (1) whether long-period phases emerge from the phase boundaries (in Figs. 9 and 10), along which the ground state is infinitely degenerate.

III. MEAN-FIELD THEORY

To obtain the phase diagram of model (1) in the mean-field approximation, we assume that the density matrix of this model can be written as a product over single-site and single-link density matrices. We then use a standard variational method" to obtain the function

$$
\begin{aligned}
F(\{s_i\},\{t_{ij}\}) = & -H\sum_i s_i - J\sum_{\langle i,j\rangle} s_i s_j - \mu\sum_{\langle i,j\rangle} t_{ij} - V\sum_{\langle ij,ik\rangle} t_{ij}t_{ik} - V_1\sum_{\langle\langle ij,ik\rangle\rangle} t_{ij}t_{ik} \\
& - J_1\sum_{\langle i,j\rangle} s_i s_j t_{ij} + \frac{k_B T}{2}\sum_i \left[(1+s_i)\ln\left[\frac{1+s_i}{2}\right] + (1-s_i)\ln\left[\frac{1-s_i}{2}\right]\right] \\
& + k_B T\sum_{\langle i,j\rangle}[t_{ij}\ln t_{ij} + (1-t_{ij})\ln(1-t_{ij})] \ , \qquad (3)
\end{aligned}
$$

which, when minimized with respect to the order parameters $\{s_i\}$ and $\{t_{ij}\}$, yields the mean-field equations for these order parameters. The values of s_i and t_{ij} at the lowest minimum of F yield the mean-field values of $M_i\equiv\langle\sigma_i\rangle$ and $A_{ij}\equiv\langle\tau_{ij}\rangle$ (the angular brackets denote thermal averages) and $F_{\rm MF}(T,H,J,\mu,V,V_1,J_1)\equiv F(\{M_i\},\{A,\})$ the corresponding, mean-field free energy. The loci of nonanalyticities of $F_{\rm MF}$ yield the mean-field phase boundaries in the six-dimensional space of the parameters $T, H, \mu, V, V,,$ and J_1 ($J=1$).

Note that we make no assumptions about the spatial variations of the order parameters s_i and t_{ij}. This is in contrast to some mean-field studies of other lattice models for oil-water-surfactant mixtures. In these studies, the authors assumed that the order parameters vary periodically in space; in addition, they almost always assume that the order parameters vary along only one spatial direction.

In Sec. II we noted that (for $V_1=0$ or $H=0$) the problem of minimizing $\mathcal{H}$ with respect to $\{\sigma_i\}$ and $\{\tau_{ij}\}$ reduces to the problem of minimizing the energy of the finite clusters shown in Fig. 8; the ground-state configuration of the σ_i's and τ_{ij}'s in model (1) follows by a periodic repetition of the lowest-energy configuration of these clusters. This occurs because the lowest-energy configurations of contiguous clusters are not frustrated with respect to each other (this would not necessarily be true were $V_1\neq0$ or $H\neq0$). The application of the method of Karl[68] similarly reduces the problem of minimizing F [Eq. (3)] with respect to $\{s_i\}$ and $\{t_{ij}\}$ to the problem of minimizing F defined for small clusters (Fig. 8). This is true for $V_1=0$ or $H=0$, *and at the level of the mean-jield approximation,* it follows rigorously that, at the lowest minimum of F, M_i and A_{ij} are periodic with period at most four and the resulting phases are either lamellar or superantiferromagnetic in $d=2$. Therefore, within mean-field theory, we must have both V_1 and H nonzero to obtain long-period or completely inhomogeneous, thermodynamically stable phases.

For the case V_1, $H\neq0$, we obtain solutions to the mean-field equations for $\{s_i\}$ and $\{t_{ij}\}$ only for $d=2$. This infinite set of coupled, nonlinear equations reduces to a finite set for periodic solutions. We look for lamellar solutions (along $\langle10\rangle$ or $\langle11\rangle$ lines), with period up to 10, and superantiferromagnetic solutions, with unit cells as large as 6×6 and sides along $\langle10\rangle$ or $\langle11\rangle$ lines. To investigate the existence of completely inhomogeneous solutions, we look for solutions to the mean-field equations for all the variables $\{s_i\}$ and $\{t_{ij}\}$ on a 32×32 lattice with periodic boundary conditions. We use an iteration method to obtain solutions of these equations. For this 32×32 lattice, we start from various random configurations.

Figures 11(a) and 11(b) show representative, two-

dimensional sections through the mean-field phase diagram of model (1), with $d=2$, $J=1$, $V_1=0$, and $H=0$. The phases shown in the zero-temperature phase diagram of Fig. 9(a) remain thermodynamically stable at low temperatures. They coexist with each other along the first-order phase boundaries (solid lines) shown in Figs. 11(a) and 11(b). There are some exceptions: Since the zero-temperature phase boundary between the phases AF1 and FS+ [marked AD in Fig. 9(a)] is infinitely degenerate (infinitely many phases have the same energy along AD) at any finite temperature $T>0$, the transition from AF1 to FS+ occurs via a sequence of two continuous transitions: AF1-P followed by P-FS+. As the temperature increases, these low-temperature phases either (a) become one phase at a critical point, as is the case with the ferromagnetic phases F+ and FS+, or (b) evolve via first-order or second-order (dashed lines) transitions into the disordered paramagnetic phase P. Solid circles denote tricritical points where first-order boundaries meet second-order (ordinary critical) lines. Note in particular that three-phase coexistence between the phases P, $F+$, and F− is obtained for some values of J_1. [This first-order boundary is actually a triple line; it develops into first-order planes when $H\neq 0$; along these planes the phase P coexists with $F+$ ($F-$) if $H>0$ ($H<0$).] This coexistence between P, F+, and $F-$ (which we interpret as O-W-$\mu\epsilon$ coexistence in Sec. IV) persists even when we include the fluctuations that mean-field theory ignores; however, these fluctuations reduce the length of the first-order phase boundary by a large amount; and they yield microstructures in the paramagnetic phase P that are similar to microemulsion microstructures. (At the mean-field level the paramagnet P is completely structureless: $M_i=0$ for all i.) We elaborate on some technical points below.

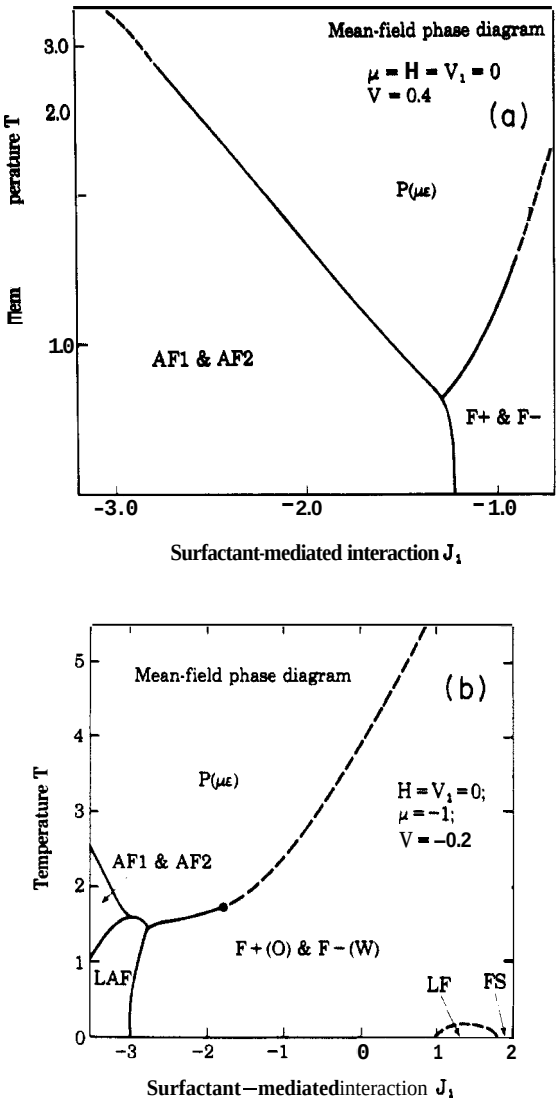

FIG. 11. Mean-field phase diagram for model (1) in $d=2$ obtained as described in the text. Solid lines represent first-order phase boundaries; dashed lines indicate critical lines. Closed circles denote tricritical points (a) $\mu=H=V_1=0$ and $V=0.4$. Note the three-phase coexistence of the microemulsion, water-rich, and oil-rich phases along one of the first-order boundaries. (b) $H=V_1=0$, $\mu=-1.0$, and $V=-0.2$. Note the coexistence of lamellar, ferromagnetic, and paramagnetic phases. All energies and the temperature are in units of $J\equiv 1$.

The first-order phase boundary between the phases $F+$ and FS+ does not show up on the scale of Figs. 11(a) and 12(a); however, it is shown in the schematic phase diagram of Fig. 5. The nature of the $F+$-FS+ transition is easy to understand: it occurs at such low temperatures that the Ising spins σ_i can be set equal to 1 in model (1); the resulting Hamiltonian for the variables τ_{ij} is just a lattice-gas model that is equivalent to an Ising model. Thus the F+-FS+ first-order transition is like the ferromagnetic-up to ferromagnetic-down transition in the Ising model.

In the vicinity of the point A we find (in mean-field theory) the following sequence of transitions: $P_1 \rightarrow F+ \rightarrow P$ as the temperature is lowered; both P_1 and P_2 are paramagnetic phases, but the latter has a much higher density of surfactant molecules than the former. Equilibration problems have prevented us from checking whether this sequence of transitions persists when we do Monte Carlo simulations of model (1).

It is easy to understand the mechanism that leads to the triple line along which P-F+-F− (i.e., $\mu\epsilon$-O-W) coexistence occurs: We expand the variational function F [Eq. (3)] about $s_i=0$ and $t_{ij}=\frac{1}{2}$, retain terms to order $(t_{ij}-\frac{1}{2})^2$, and then eliminate the t_{ij}'s (via, say, a summation over the t_{ij}'s, which is possible because the integrals are Gaussian). This elimination of the t_{ij}'s yields an effective variational function F_{eff} with a quartic term in s_i whose coefficient is $T/12-J_1^2/4T$. For $|J_1|>T/\sqrt{3}$, this coefficient can be negative and leads to a first-order boundary along which three phases coexist; such a first-order boundary also ends in a tricritical point.

In addition to quantitative shortcomings (e.g., the overestimation of the length of the first-order phase boundary), the mean-field phase diagram of model (1) has one qualitative failing: In the limit $V=V_1=0$ and with $H=0$ and $J_1=-2J-\mu$ it follows from Eq. (2) that $J_{\text{eff}}=0$, so there can be no phase transition at any temper-

ature; however, in this limit, mean-field theory yields a nonzero transition temperature from the paramagnetic to the ferromagnetic phase.

Our mean-field theory for model (1) yields a variety of metastable phases that include long-period lamellar and superantiferromagnetic phases and disordered, glasslike phases, whose microstructures are similar to microemulsion microstructures. These metastable phases appear in the range of parameters where the ordered, low-temperature phases of Fig. 11 are thermodynamically stable.

Most of our mean-field studies have been done with $V_1=0$. However, none of our principal, qualitative results change when $V_1\neq 0$. In particular, three-phase coexistence between P, $F+$, and $F-$ phases persists even when $V_1\neq 0$. It is possible that long-period lamellar or superantiferromagnetic phases might be thermodynamically stable with V_1 and H nonzero (Sec. II); however, we have not been able to find them in our mean-field calculations in the regions of parameter space that we have explored.

IV. MONTE CARLO SIMULATIONS

We use Monte Carlo simulations to study equilibrium and some nonequilibrium statistical properties of model (1). Most of our simulations are done in the grand-canonical ensemble: the chemical potentials, not the densities, of oil, water, and surfactant molecules are held fixed. In some of our simulations we work in the canonical ensemble and hold the densities of these molecules at fixed values. In the grand-canonical simulations we use Glauber, single-spin-flip dynamics and in the canonical simulations we use Kawasaki, spin-exchange dynamics.[65] In our two-dimensional simulations we use square lattices of sizes 40 X 40 to **70** X **70;** in our three-dimensional simulations we use simple-cubic lattices of sizes 10X 10X 10 to 16X 16X 16. Typically 3000 to **7000** Monte Carlo steps per spin (MCS) suffice to obtain equilibrium; if not, we use more steps or flip clusters of spins. For example, in the vicinity of the phase boundaries where the phases P, $F+$, $F-$, AF1, and AF2 coexist with each other, equilibration is greatly facilitated by flipping a spin σ_i at site i along with all the link variables τ_{ij} that emerge from that site.[72] We use the leading terms in low-temperature expansions to decide which clusters of spins to flip in various regions of our parameter space.

In our simulations, we monitor the mean values of the order parameters that characterize the simple uniform and periodic phases shown in Figs. 9 and 10, obtain typical configurations of σ_i's and τ_{ij}'s to study microstructures in different phases, and, in $d=2$, we also calculate the structure factor $S(\mathbf{q})$. We also make rough estimates of the time (measured in MCS) for which a droplet retains its identity in the microemulsion phase (see below).

Figures 12(a) and 12(b) show representative, two-dimensional sections through the phase diagram of model (1). We obtain these phase diagrams from our Monte Carlo simulations. Parameters for Fig. 12(a) [Fig. 12(b)] are the same as for the mean-field phase diagram of Fig. 11(a) [Fig. 11(b)]. Of course, our Monte Carlo phase diagrams are far more accurate than their mean-field counterparts.

The phase diagram of Fig. 12(a) is qualitatively similar to its mean-field analog Fig. 11(a). In particular, the three-phase coexistence of most interest to us, namely, the coexistence of the phases P, $F+$, and $F-$ along the first-order boundary, appears in both Figs. 11(a) and 12(a). Our simulations yield microstructures, like those of microemulsions [Figs. 1(c)–1(e)], for the phase P (see

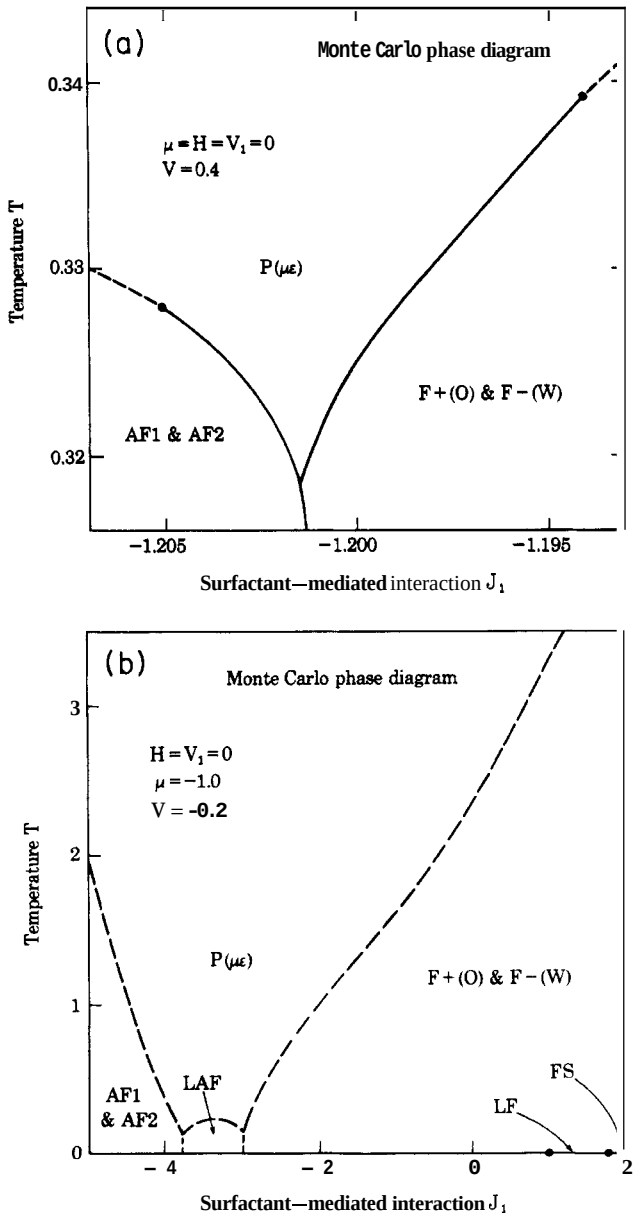

FIG. 12. Monte Carlo phase diagrams for **model** (1) **with the same values of the parameters as in Fig.** 11. **Again solid lines indicate first-order phase boundaries and dashed lines denote continuous transitions. (a)** $\mu=H=V_1=0$ **and** $V=0.4$. **Note the scale on the abcissa** (J_1). **The transition temperatures are lower and the** O-W-$\mu\epsilon$ **coexistence line is much shorter compared to the mean-field results** of **Fig.** 11(a). (b) $H=V_1=0$, $\mu=-1.0$ **and** $V=-0.2$. **Lamellar phases appear in this region.**

below); thus we identify P as a microemulsion phase and conclude that our model (1) shows O-W-$\mu\epsilon$ (i.e., F+-F—-P) coexistence. Our simulations indicate that this qualitative property of the model persists[73] even when $d = 3$ or $V_1 \neq 0$. Indeed, we find that small and positive (i.e., attractive) V_1 leads to an enhancement of the length of the first-order boundary (by approximately a factor of 2). Also, simulations of the three-dimensional version of the model with $V_1 = 0$ produce a three-phase coexistence line of length comparable to that found in two dimensions.

Not surprisingly, the fluctuations that are present in our Monte Carlo simulations, but not in our mean-field calculations, lead to far lower transition temperatures in Fig. 12(a) than in Fig. 11(a). These fluctuations also reduce drastically the length of first-order phase boundaries [cf. Figs. 12(a) and 11(a)]. By changing the parameter V and V_1 the length of this phase boundary can be increased or decreased; however, in our Monte Carlo simulations, we have not found any values of V and V_1 for which this phase boundary is very long [at most twice the length it has in Fig. 12(a)]. Thus, in our model (1), O-W-$\mu\epsilon$ coexistence always occurs in the vicinity of a tricrtical point [solid circle in Fig. 12(a)]; it follows, therefore, that the interfacial tensions between any two of these coexisting phases must be very low.[64] Fluctuations also remove some of the qualitative shortcomings of our mean-field phases diagram (Sec. III): In particular, our simulations yield no phase transition, when $V = V_1 = 0$, $J_, = -2J - \mu$, and $H = 0$, in agreement with exact results (Sec. II).

The phase diagram of Fig. 12(b) and its mean-field analog Fig. 11(b) show the region of parameter space where the lamellar phases of model (1) are thermodynamically stable. The mean-field phase diagram [Fig. 11(b)] shows first-order phase boundaries along which paramagnetic, ferromagnetic, and lamellar phases coexist; because of equilibration problems, we cannot tell whether such first-order phase boundaries also appear in the Monte Carlo phase diagram [Fig. 12(b)]. Otherwise these two phase diagrams are qualitatively similar. Note, in particular, the coexistence between lamellar (L) and microemulsion ke., P) phases as seen in experiments (Fig. 2).

In Figs. 4 and 13 we show the microstructures of the paramagnetic phase P in different regions of our parameter space for $d = 2$. These microstructures are of the sort that we expect in microemulsion ($\mu\epsilon$) phases: there are large regions of water (squares) and oil (empty spaces) with surfactant molecules (lines) at oil-water interfaces. Thus it is natural to identify the paramagnetic phase P of model (1) as a microemulsion. Even at low temperatures [roughly a tenth of the temperature at which oil and water would mix in the absence of surfactant molecules[74] in model (1)], there is a rich variety of possible microstructures. Compact clusters, roughly circular (Fig. 4) or stringy [Fig. 13(a)], the analogs of roughly spherical or cylindrical clusters for $d = 3$, form when the concentrations of oil and water are sufficiently different. With roughly equal amounts of oil and water [Fig. 13(b)], the patches of oil and water are large and connected.'' Simulations on the three-dimensional model with roughly equal amounts of oil and water produce a bicontinuous structure in the sense that both the oil clusters and the water clusters percolate. (We have checked this with an explicit calculation.)

There is one unphysical feature in our microemulsion phase in the region of parameter space where we obtain O-W-$\mu\epsilon$ coexistence in model (1): this phase has a far higher density (sometimes as large as 80%) of surfactant molecules than is found in laboratory microemulsions (where it can be as low as 5%). We believe this unphysical feature arises because the relative molecular size in

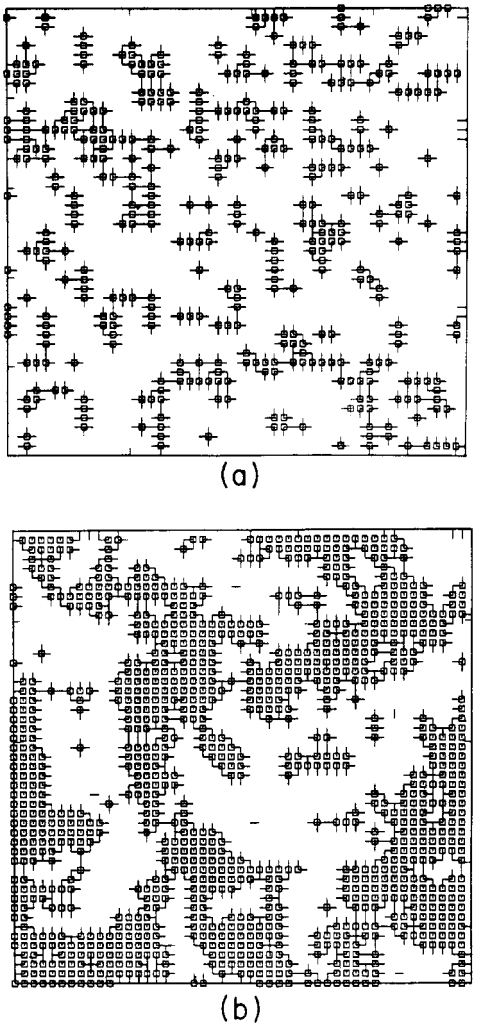

FIG. 13. Representative microstructures in the microemulsion phase from Monte Carlo simulations in $d = 2$ for (a) $V_1 = 0$, $\mu = -1.0$, $H = -0.05$, $V = -0.1$, $J_1 = -3.0$, and $T = 0.14$ and (b) $V_1 = \mu = H = 0$, $V = -0.1$, $J_1 = -1.8$, and $T = 0.33$; in both cases, $J = 1$ and T is approximately 10% above the transition temperature. Note that the clusters in (a) are stringy in contrast to the compact, roughly circular ones in Fig. 4 in another region of parameter space. In (b), the microstructure has large, connected patches of oil and water and is the analog of the $d = 3$ bicontinuous structure. Note that a bicontinuous structure is not possible in two dimensions (Ref. 75).

the model is not realistic. In fact, a crude rescaling of the size of the water regions by the ratio of the surfactant length to the water-molecule length leads to much more reasonable results. It is also possible that long-ranged interactions such as van der Waals forces play a role.

To characterize percisely the nature of the microemulsion phase of model (1), we compute the structure factor $S(\mathbf{q})$. (The structure factor we calculate is the Fourier transform of the spin-spin correlation function $\langle \sigma_i \sigma_j \rangle$; the analogous experimental quantity is the partial, oil-water structure factor.) The structure factor corresponding to the microstructure of Fig. 13(b) is shown in Fig. 6. At large values of $q \equiv |\mathbf{q}|$, $S(\mathbf{q})$ has peaks that signal the incipient antiferromagnetic ordering in model (1)(Fig. 5). We have not found peaks in $S(\mathbf{q})$ at small, but finite, values of q as are found in some experiments [Fig. 3(b)]. The structure factor of Fig. 6 has a peak at $q = 0$ which is very similar to the peak in $S(\mathbf{q})$ for a simple Ising model. However, $S(\mathbf{q})$ for the zero-field, two-dimensional Ising model, at a temperature 10% above its critical temperature, is somewhat narrower than the structure factor of Fig. 6.

Microstructures of the paramagnetic phase of an Ising model (at temperatures 5–10% above the critical temperature) are also similar to the microstructures of the paramagnetic phase of model (1). The two-dimensional Ising model yields microstructures like Fig. 13(b), and the three-dimensional Ising model yields bicontinuous microstructures. The principal difference between the microstructures of the paramagnetic phases of the Ising model and our model is the following: elementary units, such as droplets or bicontinuous networks, retain their identities far longer (a factor of 10^5–10^6) in the microemulsion phase ($\mu\epsilon$ or P) of model (1) than in the paramagnetic phase of the Ising model.[76] (For a meaningful comparison of mean droplet lifetimes, we must use the same Monte Carlo dynamics for both models. In our simulations we use single-spin-flip Glauber dynamics.) Even though our Monte Carlo dynamics is not a good representation of the dynamics of oil-water-surfactant mixtures,[77] we believe the large enhancement of droplet lifetimes in the paramagnetic phase of model (1) (relative to Ising-model droplets) is similar to the large enhancement of droplet lifetimes in laboratory microemulsion (relative to microscopic relaxation times in simple liquids). One reason for enhanced droplet lifetimes is simple: The addition of surfactant molecules to a mixture of oil and water reduces drastically the temperature at which oil and water can mix in the absence of surfactant molecules[74] [the reduction factor is nearly 10 in model (1)]; at these reduced temperatures, the dynamics is slow. The only reason this slow dynamics does not prevent us from obtaining equilibrium properties of model (1) is because we use multispin flips while calculating these properties.

Our model exhibits various metastable phases, which can be lamellar, superantiferromagnetic, or inhomogeneous (glasslike). In mean-field theory (Sec. III), these metastable phases appear as configurations of $\{s_i\}$ and $\{t_{ij}\}$ that are *local,* but not global, minima of F [Eq. (3)]. In our Monte Carlo simulations, such phases have very long lifetimes at low temperatures. Precisely how long they last depends on the details of the Monte Carlo dynamics we use. We must be cautious in associating the results of our Monte Carlo dynamics with the dynamics of oil-water-surfactant mixtures; nevertheless, it is tempting to associate the glasslike, metastable phases of our model with the glasslike phases seen in experiments[13,42] on oil-water-surfactant mixtures.

V. CONCLUSIONS

In Sec. I we have listed the principal results of our study of model (1) and in subsequent sections we have given the details of this study. Here we discuss the limitations of our model and end with a critique of other theories that emerges from our study.

Model (1) has various limitations, so it is not surprising that it does not obtain all the experimental properties of oil-water-surfactant mixtures, which we discussed in Sec. I. We list below the discrepancies between the results of our model and the results of experiments.

(1) Our model does not exhibit the large variety of long-period, lamellar phases and complicated cubic phases[8–11] seen in experiments; however, our model exhibits low-period, lamellar, and superantiferromagnetic phases which may or may not be of experimental relevance.

(2) Our model does not exhibit a lower consolute point at which microemulsions with high and low densities of droplets (of oil in water) mix and become one microemulsion phase.[16]

(3) We have not been able to find a region in the paramagnetic phase (i.e., microemulsion phase) of model (1) where the structure factor $S(\mathbf{q})$ exhibits a peak at small q ($\neq 0$) as seen in some experiments.[31–33]

(4) In the region of parameter space where we obtain O-W-$\mu\epsilon$ coexistence in model (1), the microemulsion has a high density of surfactant molecules in contrast to laboratory microemulsions.

Model (1) has some obvious limitations which, we believe, are responsible for the discrepancies listed above. We comment on these limitations below.

(1) Model (1) is a lattice model; however, we use it to describe mixtures of continuum fluids. Thus the physically relevant phases of model (1) are those in which the order parameters $\{s_i\}$ and $\{t_{ij}\}$ vary slowly on the scale of the lattice spacing. Hence, low-period lamellar and antiferromagnetic phases (e.g., LAF1 and AF1 in Figs. 9) are, most probably, artifacts of the model.

(2) Like all Ising-lattice-gas models, model (1) treats oil and water molecules on the same footing: The Hamiltonian $\mathcal{H}$ is invariant under $\sigma_i \rightarrow -\sigma_i$ and $H \rightarrow -H$. This leads to a symmetrical oil-water limit (formally, the limit $\mu \rightarrow -\infty$), in disagreement with experiments.[11] We therefore expect similar disagreement between the coexistence curves of our model and those observed in oil-water-surfactant mixtures.

(3) Since oil and water molecules occupy sites and surfactant molecules, links in our model, it assumes implicitly that these molecules are of comparable sizes. This assumption is clearly false. This could account for the

large density of surfactant molecules in the microemulsion phase of our model near 0-W-$\mu\epsilon$ coexistence. Also the structures and lattice spacings of periodic phases are determined primarily by the sizes and shapes of constituent molecules, and hence we cannot expect our model to describe accurately the details of periodic phases of oil-water-surfactant mixtures (Sec. I). Further, we do not include longer-ranged interactions, which must be present in oil-water-surfactant mixtures. Our neglect of these interactions may be responsible for the absence of long-period lamellar phases in our model. The presence of competing interactions as in the three-dimensional axial next-nearest-neighbor Ising (ANNNI) model leads to long-period lamellar phases. In Refs. 55 and 59, such phases occur precisely by this mechanism. Whether this is indeed the cause in real microemulsions is not clear. Finally, since we assume that surfactant molecules are structureless (they have neither heads nor tails), it is unlikely that our model can display lower consolute points of the sort seen in oil-water-surfactant mixtures (Sec. II).

We are studying a generalization of model (1) that does not suffer from the limitations described above. In particular, this generalized model displays a lower consolute point in the pure water-surfactant limit.

All lattice models of oil-water-surfactant mixtures suffer from most, if not all, the limitations of our model (1). However, out study of model (1) is far more detailed than the studies of all these lattice models with the exception of that of Larson *et al.*[44] None of these lattice models has, again with the exception of Ref. 44, been studied via Monte Carlo simulations like those we use to study model (1); in our mean-field study, we make no assumptions about how the order parameters vary in space. Thus, in spite of the limitations of our model (1), we believe our detailed study of it brings out certain points of principle that contrast with the results of some other studies: (1) A microemulsion phase is most naturally interpreted as a ***disordered*** phase (like a paramagnet). No simple ansatz can be made for the spatial variations of the oil, water, and surfactant densities in this phase. (2) In the microemulsion phase of our model, droplets of oil and water have neither **a** well-defined shape nor a well-defined size. It is possible that droplets with compact sizes and well-defined shapes may obtain in the microemulsion phases of models in which molecular structures and interactions are treated more accurately than in our model. Nevertheless, we find it hard to justify the use of the droplet size as an order parameter for a microemulsion phase. Also, we believe it is very unlikely that the free energy exhibits any nonanalytic behavior (such as discontinuous first derivatives) when droplets in a microemulsion phase change from roughly spherical to roughly cylindrical shapes; thermodynamic functions might show rapid crossover behavior, but ***not*** a thermodynamic phase transition. Controversies about the points of principle that we have raised in this paper can only be settled by studying models of oil-water-surfactant mixtures via detailed calculations like ours and by systematic experimental investigations.

ACKNOWLEDGMENTS

We thank M. Barma, R. Goldstein, J. S. Huang, M. D. Lipkin, T. V. Ramakrishnan, S. Trugman, and especially Y. He and B. Widom for useful discussions. One of us (R.P.) thanks the Department of Science and Technology (India)and the University Grants Commission (India)for support and the Department of Physics, The Ohio State University, for hospitality while most of this work was being done. Support from the National Science Foundation, through Grant Nos. DMR 8451922 and DMR 8404961, is gratefully acknowledged.

---

[1] K. Chen, C. Ebner, C. Jayaprakash, and R. Pandit, J. Phys. C ***20,*** L361 (1987).

[2] ***Micellization, Solubilization, and Microemulsions,*** edited by K. L. Mittal (Plenum, New York, 1977), Vol. 2.

[3] ***Physics of Amphiphiles: Micelles, Vesicles, and Microemulsions,*** edited by V. Degiorgio and M. Corti (Academic, New York, 1985).

[4] ***Microemulsion Systems; Surfactant Science Series,*** edited by H. L. Rosano and M. Clausse (Dekker, New York, 1987), Vol. 24.

[5] P. G. de Gennes and C. Taupin, J. Phys. Chem. **86,** 2294 (1982).

[6] Often more than three components are required to solubilize one component (oil) in the other (water). The fourth component is called a cosurfactant; a typical example is butanol [in a mixture of toluene (oil), water, and sodium dodecyl sulfate (surfactant)]. The fifth component is often an electrolyte (sodium chloride in the preceding example). We restrict ourselves to three-component mixtures.

[7] For recent measurements, see, e.g., D. Langevin, D. Guest, and J. Meunier, Colloids Surf. **19,** 159 (1986).

[8] For a recent study of such lamellar phases, see F. C. Larche, J. Appell, G. Porte, P. Bassereau, and J. Marignan, Phys. Rev. Lett. **56,** 1700 (1986).

[9] B. Lindman in Ref. 3, pp. 7–23.

[10] K. Fontell, P. Ekwall, L. Mandell, and K. Fontell, J. Colloid Interface Sci. 33, 215 (1979).

[11] Lamellar, hexagonal, and cubic phases can also occur when oil is absent. See G. J. T. Tiddy, Phys. Rep. **57,** 1 (1980).

[12] L. E. Scriven, in Ref. 2, p. 877.

[13] D. R. MacFarlane, I. R. McKinnon, E. A. Hildebrand, and C. A. Angell, in Ref. 4, pp. 311–318, and references cited therein.

[14] M. Kahlweit, R. Strey, and D. Haase, J. Phys. Chem. ***89,*** 163 (1985); M. Kahlweit and R. Strey, Angew. Chem., Int. Ed. Engl. **24,** 654 (1985).

[15] E. W. Kaler, H. T. Davis, and L. E. Scriven, J. Chem. Phys. ***79, 5685*** (1983), and references therein.

[16] A. M. Cazabat, D. Langevin, J. Meunier, and A. Pouchelon, Adv. Colloid Interface Sci. **16,** 175 (1982), and references therein.

[17] P. Bothorel in Ref. 3, pp. 702–722, and references therein.

[18]D. Roux and A. M. Bellocq, in Ref. 3, pp. 842–856.
[19]A. A. Calje, W. G. M. Agterof, and A. Vrij, in Ref. 2, pp. 779–790.
[20]A. Graciaa, J. Lachaise, P. Chabrat, L. Letamendia, J. Rouch, C. Vaucamps, M. Bourrel, and C. Chambu, J. Phys. (Paris), Lett. 38, L-253 (1977);39, L-235 (1978).
[21]M. Zulauf and H. F. Eicke, J. Phys. Chem. 83,480 (1979).
[22]E. Gulari, B. Bedwell, and S. Alkhaji, I. Colloid Interface Sci. 77, 202 (1980).
[23]A. M. Cazabat, D. Chatenay, D. Langevin, and J. Meunier, Faraday Discuss. Chem. Soc. 76, 291 (1982).
[24]D. Guest and D. Langevin, J. Colloid Interface Sci. 112, 208 (1986).
[25]J. H. Schulman, W. Stockenius, and L. M. Prince, J. Phys. Chem. 63, 1677 (1959).
[26]E. W. Kaler, K. E. Bennet, H. T. Davis, and L. E. Scriven, J. Chem. Phys. 79,5673 (1983).
[27]L. Auvray, J. P. Cotton, R. Ober, and C. Taupin, J. Phys. (Paris),45, 913 (1984).
[28]D. J. Cebula, R. H. Ottewil, and J. Ralston, J. Chem. Soc., Faraday Trans. 177,2585 (1981).
[29]A. M. Cazabat, in Ref. 3, pp. 723–756.
[30]J. B. Hayter, R. H. Ottewil, and P. N. Pusey, in Ref. 3, pp. 793–801.
[31]A. DeGeyer and J. Tabony, Chem. Phys. Lett. 113, 83 (1985).
[32]M. Kotlarchyk, Physica 136B, 274 (1986).
[33]L. Auvray, J. P. Cotton, R. Ober, and C. Taupin, Physica 136B, 281 (1986).
[34]See Ref. 27; see also J. B. Hayter, in Ref. 3, pp. 59–93, especially pp. 66–71.
[35]D. Quemada and D. Langevin, J. Theor. Appl. Mech., numero special, 201 (1985).
[36]P. Guering and B. Lindman, Langmuir 1,464 (1985).
[37]For related but slightly different points of view see Refs. 23 and 32.
[38]J. Appell and G. Porte, J. Phys. (Paris), Lett. 44, L-689 (1983).
[39]This possibility has been suggested on the basis of a phenomenological theory by S. A. Safran, L. A. Turkevich, and P. Pincus, J. Phys. (Paris),Lett. 45, L-69 (1984).
[40]There is some evidence for the formation of long-lived aggregates of droplets in micromulsions: See P. Guering, A. M. Cazabat, and M. Paillette, Europhys. Lett. 2,953 (1986).
[41]J. P. Hansen and I. R. McDonald, ***Theory of Simple Liquids*** (Academic, New York, 1976), pp. 212 and 213.
[42]S. H. Chen and J. S. Huang, Phys. Rev. Lett. 55, 1888 (1985).
[43]A. Robledo, C. Varea, and E. Martina, J. Phys. (Paris) Lett. 46, L-967 (1985).
[44]R. G. Larson, L. E. Scriven, and H. T. Davis, J. Chem. Phys. 83,2411 (1985).
[45]E. Ruckenstein, in Ref. 2, pp. 755–778.
[46]Y. Talmon and S. Prager, J. Chem. Phys. 69,2984 (1978).
[47]J. Jouffroy, P. Levinson, and P. G. deGennes, J. Phys. (Paris) 43, 1241 (1982).
[48]B. Widom, J. Chem. Phys. 81, 1030 (1984); Langmuir 1, (1985).
[49]P. Balbuena, C. Borzi, and B. Widom, Physica 138A, *55* (1986).
[50]C. Borzi, R. Lipowsky, and B. Widom, J. Chem. Soc. Faraday Trans. 2 82, 1739 (1986).
[51]R. E. Goldstein, J. Chem. Phys. 84, 3367 (1986), especially Sec. V.
[52]S. A. Safran and L. A. Turkevich, Phys. Rev. Lett. **50,** 1930 (1983).
[53]S. A. Safran, D. Roux, M. E. Cates, and D. Andelman, Phys. Rev. Lett. 57,491 (1986);(unpublished).
[54]W. R. Rossen, R. G. Brown, S. Prager, L. E. Scriven, and H. T. Davis, Soc. Pet. Eng. J. 22,945 (1982).
[55]B. Widom, J. Phys. Chem. 88, 6508 (1984);J. Chem. Phys. 84, 6943 (1986).
[56]B. Widom, K. A. Dawson, and M. D. Lipkin, Physica 140A, 26 (1986), and references therein to the work of their group.
[57]A. Robledo, Europhys. Lett. 1,303 (1986).
[58]C. Varea and A. Robledo, Phys. Rev. A 34,2760 (1986).
[59]M. Schick and W.-H. Shih, Phys. Rev. B 34, 1797 (1986); Phys. Rev. Lett. 59, 1205 (1987). Note that in the first paper these authors interpreted a lamellar phase as a microemulsion phase while in the second an isotropic phase is so identified in agreement with our earlier paper, Ref. 1.
[60]M. Teubner (unpublished).
[61]S. Alexander, J. Phys. (Paris),Lett. 39, L-1 (1978). In addition to the states 1 and 0 that we allow for the variables τ_{ij}, Alexander also allows the state $\tau_{ij} = -1$, in which a surfactant molecule occupies a link in between oil and water molecules but with its hydrophilic head towards the oil molecule and its hydrophobic tail towards the water molecule. The inclusion of this state does not lead to three-phase coexistence between P, $F+$, and $F-$ phases (Fig. 7) along a first-order phase boundary. In our model, the state $\tau_{ij} = -1$ is assigned an infinite energy.
[62]Coarse-grained phenomenological theories (such as the theory of Ref. 52) begin with an effective droplet-droplet interaction; they cannot, of course, obtain such an interaction from a microscopic theory that would explain the underlying cause of critical points in microemulsion phases (Ref. 16). Simple droplet-droplet interactions have been proposed by D. Roux, A. M. Bellocq, and P. Bothorel, in ***Surfactants in Solution,*** edited by K. L. Mittal and B. Lindman (Plenum, New York, 1984), Vol. 3, pp. 1843–1865.
[63]At atmospheric pressure, either water or the oil or both boil before they mix; however, boiling can be suppressed by the application of pressure.
[64]In the vicinity of a critical (multicritical) point, the interfacial tension σ approaches zero as $(T_c - T)^{(d-1)\nu}$, where T_c is the critical (multicritical)temperature, d the dimension, and ν the correlation-length exponent in the vicinity of this critical (multicritical)point.
[65]K. Binder, in ***Monte Carlo Methods In Statistical Physics,*** edited by K. Binder (Springer, New York, 1979), pp. 1–45.
[66]For the equivalence of the Ising model to a lattice-gas model, see K. Huang, ***Statistical Mechanics*** (Wiley, New York, 1963), pp. 332–336; ibid. pp. 349–373, for the Onsager solution of the two-dimensional Ising model.
[67]Note that Alexander does not identify the phases in his model in the way we do. In particular, he does not identify the paramagnetic phase as a microemulsion.
[68]G. Karl, Phys. Rev. B **7,** 2050 (1973).
[69]This annealing procedure entails equilibrating our lattice-gas model at a high temperature and then cooling it slowly to low temperatures in such a way that the system attains equilibrium at all temperatures it passes through. The state of the system at very low temperatures gives a nearly defect-free ground state. Of course, the ground state found thus may not be the true ground state but only a very-long-lived metastable state.
[70]See, e.g., M. E. Fisher and W. Selke, Philos. Trans. R. Soc. London 302, 1 (1981).
[71]H. Falk Am. J. Phys. 38, 858 (1970).
[72]Some care must be exercised while making such multispin

flips. Even if such a flip satisfies the condition of detailed balance (Ref. 65), it may lead to nonergodic behavior: Given an initial microstate, it may not be possible to get to another by any sequence of the above multispin flips. To avoid this problem, we follow a multispin pass through the lattice by a single-spin-flip pass, in which only one site or link variable is flipped.

[73] Our earlier Monte Carlo calculations (Ref. 1) were inconclusive (with regard to first-order O-W-$\mu\epsilon$ coexistence) with $V_1 \neq 0$ because of equilibration. Our current, longer Monte Carlo simulations show that this first-order coexistence persists also when $\mathbf{k}', \neq 0$.

[74] At high temperatures, oil and water would mix in our model (1). This situation is not often realized in the laboratory at atmospheric pressure (Ref. 63).

[75] Bicontinuous phases cannot form for $d = 2$ because there can be only one percolating cluster in this case; see, e.g., V. K. S. Shante and S. Kirkpatrick, Adv. Phys. **20,** 325 (1971).

[76] At $T = 1.1 T_c$ in the Ising model ($H = 0$) such droplets retain their identities for 20–100 MCS. We define the mean droplet lifetime as the time for which a droplet changes its size by 50%; we allow for droplet translations.

[77] For a good representation we must build in all the conservation laws (e.g., densities of oil, water, and surfactant molecules are conserved in experiments) and hydrodynamic effects; see, e.g., P. C. Hohenberg and B. I. Halperin, Rev. Mod. Phys. 49,435 (1977).

[78] N. D. Mermin and J. Rehr, Phys. Rev. Lett. **26,** 957 (1971); Phys. Rev. A 4, 2408 (1971).

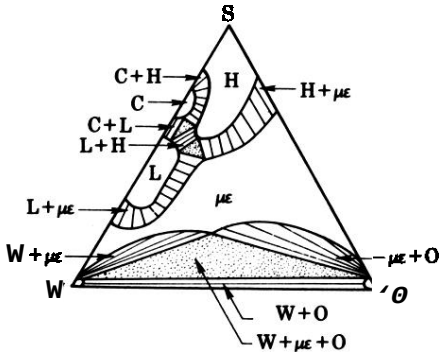

FIG. 2. Schematic phase diagram for an oil-water-surfactant $(O\text{-}W\text{-}S)$ mixture in the composition triangle at fixed temperature. Unshaded areas represent single-phase regimes, areas hatched with tie lines indicate regions of two-phase coexistence, and dotted areas denote three-phase coexistence regions. Oil-rich, water-rich, microemulsion $(\mu\epsilon)$, lamellar (L), hexagonal (H), and cubic (C) phases are shown. In laboratory mixtures all these phases might not coexist as shown at one temperature; furthermore, different types of cubic, hexagonal, and lamellar phases might occur. The microstructure of the $\mu\epsilon$ phase varies from the oil-in-water type [Fig. 1(c)] near the water-rich comer, through the bicontinuous type [Fig. 1(e)] in the middle of the triangle, to the water-in-oil type [Fig. 1(d)] near the oil-rich comer.

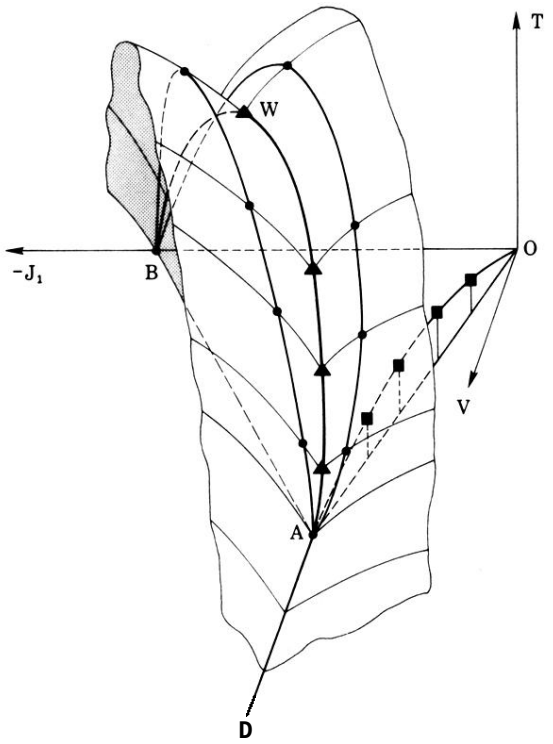

FIG. 5. Schematic phase diagram in two dimensions in V, J_1, and T space for $J > 0$, $V > 0$, $J_1 < 0$, $V_1 = 0$, and $H = 0$. Points O, A, B, and D are as in Fig. 9(a). There is a sheet of first-order transitions between the F and AF phases bounded by AB and the line of triple points (▲). Two sheets of first-order transitions branch off from the line (▲) and become sheets of critical phase transitions at the tricritical lines (●). These sheets separate the AS and F regions from the paramagnetic or microemulsion phase P at higher T; they drop to $T = 0$ on the line AD. Finally, there is a sheet of first-order transitions between the F and FS phases [see Fig. 9(a)] and bounded by the line OA and the line of critical points (■). The latter lies below the phase P everywhere except at A.